Title	Loading effect on swelling of nematic elastomers
Author(s)	Urayama, K; Mashita, R; Kobayashi, I; Takigawa, T
Citation	JOURNAL OF CHEMICAL PHYSICS (2007), 127(14)
Issue Date	2007-10-14
URL	http://hdl.handle.net/2433/50064
Right	Copyright 2007 American Institute of Physics. This article may be downloaded for personal use only. Any other use requires prior permission of the author and the American Institute of Physics.
Type	Journal Article
Textversion	publisher; none

Loading effect on swelling of nematic elastomers

Kenji Urayama[a] and Ryo Mashita
Department of Materials Chemistry, Kyoto University, Kyoto 615-8510, Japan

Ichiro Kobayashi
Electronic Materials Research Laboratories, Nissan Chemical Industries, Chiba 274-0052, Japan

Toshikazu Takigawa
Department of Materials Chemistry, Kyoto University, Kyoto 615-8510, Japan

(Received 2 August 2007; accepted 12 September 2007; published online 10 October 2007)

Externally imposed loading has substantially different effects on the swelling of nematic elastomers in the high-temperature isotropic and low-temperature nematic states. In the isotropic state, the stretching drives a considerably large degree of further swelling, whereas the stretching-induced volume change in the nematic state is significantly suppressed. In the isotropic phase that favors the less anisotropic state, the further swelling occurs to reduce the shape anisotropy caused by the imposed elongation. In the nematic phase, no significant swelling is induced because further swelling decreases the nematic order enhanced by the applied stretching. These different loading effects in the isotropic and nematic states observed in the experiments are qualitatively described by a mean field theory. © *2007 American Institute of Physics*. [DOI: 10.1063/1.2794333]

I. INTRODUCTION

Liquid crystal elastomers (LCEs)—first envisaged by de Gennes[1]—exhibit many interesting properties owing to their cross characters of liquid crystals and elastomers.[2–5] The physical properties of LCEs have been extensively investigated since the synthesis of monodomain LCEs having a global director (macroscopic orientation) was reported.[6] A unique characteristic of LCEs is the strong coupling of molecular orientational order and macroscopic shape. One of the most familiar phenomena stemming from this coupling is the spontaneous elongation or compression in response to temperature variations that cause a change in orientational order of mesogens. Such thermally induced deformation in the neat state was studied by many researchers.[2] We showed for the polydomain LCEs without global director that the volume (the degree of swelling) is discontinuously reduced by isotropic-to-nematic transition (nematic ordering) when they are allowed to swell in solvents.[7] The subsequent study[8] on the monodomain LCEs swollen in solvents revealed that the shape as well as the volume is strongly coupled to the orientational order: The nematic ordering induces a volume reduction together with an elongation along the director. If the solvent has nematicity, the nematic order of the surrounding solvent also influences the swelling.[9–12] These swelling behaviors are governed by the orientational orders of the constituent LCs, and they are described by a mean field theory.[13–16] The characteristic swelling dynamics was also revealed by the temperature-jump experiments.[17,18]

In the present paper, we investigate the effect of uniaxial loading on the swelling of nematic elastomers. For isotropic elastomers, the imposition of external forces (strains) on the fully swollen elastomers considerably changes the free energy, and it causes shrinkage or further swelling depending on the type of imposed fields. Such field-induced swelling (shrinking) phenomena for isotropic elastomers have been investigated under uniaxial[19–23] and biaxial[24] strains, solvent flow,[25] ultracentrifugal force,[26] and oscillating force.[27] The thermodynamics and kinetics of the field-induced swelling were well established for isotropic gels. In the case of stretching loading, the induced further swelling was observed for several isotropic gels.[19,20,27] The loading effect on the swelling of nematic elastomers is expected to differ significantly from that of isotropic elastomers, because the loading strongly affects the orientational order governing the swelling. Wang and Warner theoretically pointed out a considerable effect of loading on the phase diagrams for LCEs in nematic solvents.[14] Matsuyama and Kato also theoretically showed a pronounced effect of magnetic fields on the anisotropic swelling of LCEs.[15] Weiss and Finkelmann[28] experimentally examined how the uniaxial elongation imposed on the lyotropic LC networks affects the subsequent anisotropic swelling, but their scope is substantially different from the present issue. They elongated the unswollen or "not fully swollen" elastomers with polydomain structures, and investigated how the monodomain structure formed by the subsequent swelling was influenced by the imposed strain. In the present case, the LCEs before elogation originally have the monodomain alignment and they are in the fully swollen state. The imposed loading affects the degree of orientational order in the monodomain structure. To our knowledge, there is no corresponding experimental study. This experiment provides an important basis to understand the external-field effect on the phase diagrams of LCEs in solvents. We compare the loading effect on the reswelling of nematic elastomers in the high-temperature isotropic and low-temperature nematic states. This comparison clearly reveals

[a]Author to whom correspondence should be addressed. Electronic mail: urayama@rheogate.polym.kyoto-u.ac.jp

the difference in the loading effect from the nematic and isotropic elastomers. We also describe the loading effect on the basis of a mean field theory, and compare the experimental results with the theoretical prediction.

II. THEORY FOR SWELLING OF NEMATIC ELASTOMERS UNDER CONSTANT LOADS

In this section, we describe the mean field theory for the swelling of nematic elastomers in isotropic (nonmesomorphic) solvents under constant loads imposed along the original nematic director. The present theory is developed from the model for the free swelling in isotropic solvents without external loading.[8,13,15] The contribution of external loading to free energy is considered in the same way as that for nematic solvent systems.[14] For simplicity, the theory does not consider explicitly the interactions specific to side chain nematic networks such as the dangling mesogen-backbone polymer interaction and the effect of totally nonmesomorphic backbone on solubility. These interactions are reflected in the N–I transition temperature and/or the Flory-Huggins mixing interaction parameter. The orientational order parameters for the chain backbone (S_B) and the dangling mesogen (S) differ in general, but they can be connected through a proportional constant.[2] The simple relation $S_B=S$ is assumed here. The experimental phase diagrams for the solutions of un-cross-linked side chain nematic polymers are successfully explained by a mean field approach along the same treatments.[29,30]

We consider the nematic elastomer where each network chain contains mesogenic and nonmesomorphic monomers. The number of the segments (sites) on a single network chain (n) is given by $n=(n_m+n_s)t$, where t is the number of the repeating units, n_m and n_s are the numbers of sites occupied by the mesogenic and nonmesogenic monomers, respectively. The degree of swelling, Q, in an isotropic solvent with the axial ratio of unity is defined as the ratio of the elastomer volumes in the swollen and preparation states,

$$Q=\frac{V}{V^0}=\frac{1}{\varphi}=\frac{b^3(nN_g+N_s)}{b^3nN_g}, \tag{1}$$

where ϕ, b^3, N_g, and N_s are the volume fraction of elastomer, the volume of a unit segment, and the numbers of the network chains and the solvent molecules inside the gel, respectively. The preparation state is denoted as the superscript 0, and taken as the dry state ($\phi^0=1$) for simplicity. The anisotropic swelling of nematic elastomers with uniaxial orientation is characterized by the principal ratios λ_L and λ_T along (L) and normal (T) to the director,

$$Q=\lambda_L\lambda_T^2, \tag{2}$$

where $\lambda_L=\lambda_T=1$ in the preparation state.

The change of the total free energy density ΔF is customarily expressed as a sum of those of the free energy densities stemming from elasticity of nematic elastomer, isotropic mixing of elastomer with solvent, nematic ordering of mesogenic molecules, and external uniaxial stress (designated as F_{el}, F_{mix}, F_{nem}, and F_{ext}, respectively),

$$\Delta F=\Delta F_{\mathrm{el}}+\Delta F_{\mathrm{mix}}+\Delta F_{\mathrm{nem}}+\Delta F_{\mathrm{ext}}. \tag{3}$$

The elastic energy ΔF_{el} for nematic elastomers was derived by Warner *et al.*[2,31] as

$$\frac{\Delta F_{\mathrm{el}}}{k_BT}=\frac{\phi}{2n}\left[\frac{\lambda_L^2}{1+2S}+\frac{2\lambda_T^2}{1-S}-3-\ln\frac{1}{(1+2S)(1-S)^2}\right], \tag{4}$$

where k_B and T are the Boltzmann constant and absolute temperature, respectively, and S is the orientational order parameter of the chain backbone. Equation (4) is for nematic elastomers formed in the isotropic phase ($S^0=0$). As pointed out in Ref. 2, however, within the framework of the theory, the important characteristics such as spontaneous shape variations are unaffected by whether the elastomers are formed in the isotropic ($S^0=0$) or nematic phase ($S^0\neq 0$). To avoid the complexity, we employ the expression of ΔF_{el} with $S^0=0$. The form of ΔF_{el} with $S^0\neq 0$ is given in our previous paper.[8]

The form of ΔF_{mix} is written on the basis of the Flory-Huggins theory[32] as

$$\frac{\Delta F_{\mathrm{mix}}}{k_BT}=(1-\phi)\ln(1-\phi)+\chi\phi(1-\phi), \tag{5}$$

where χ is the Flory-Huggins parameter representing the mixing interaction between the elastomer network and the isotropic solvent, and the entropic contribution of the elastomer is zero because of the infinite molecular weight.

According to the Maier-Saupe theory[33,34] ΔF_{nem} is given by

$$\frac{\Delta F_{\mathrm{nem}}}{k_BT}=\frac{\phi_m}{n_m}\int\psi(\theta)\ln[4\pi\psi(\theta)]d\Omega-\tfrac{1}{2}\nu\phi_m^2S^2, \tag{6}$$

where ν is the Maier-Saupe interaction parameter between the mesogens proportional to reciprocal temperature, and ϕ_m is the volume fraction of mesogen given by $\phi_m=\phi n_m/(n_m+n_s)=\phi(1-p)$, with the spacer fraction $p=n_s/(n_m+n_s)$. The orientation distribution function $\psi(\theta)$ is related to S as

$$S=\int P_2(\cos\theta)\psi(\theta)d\Omega, \tag{7}$$

where θ is the angle between the chain backbone and the director, Ω is the solid angle, and $P_2(x)=(3x^2-1)/2$ is the second Legendre polynomial. The function $\psi(\theta)$ is given by

$$\psi(\theta)=\frac{1}{Z}\exp[\eta P_2(\cos\theta)], \tag{8}$$

where η is a dimensionless parameter characterizing the strength of the nematic field, and $Z=\int\exp|\eta P_2(\cos\theta)|d\Omega$ is the partition function to normalize $\psi(\theta)$.

The term ΔF_{ext} originating from the imposed uniaxial force f is written as

$$\frac{\Delta F_{\mathrm{ext}}}{k_BT}=-\frac{f\Delta l_L}{V}=-\phi\sigma(\lambda_L-1), \tag{9}$$

where Δl_L is the displacement measured from the preparation state, and σ is the nominal stress, i.e., the force per cross section in the reference (preparation) state.

The equilibrium relation between λ_L and σ is obtained by the minimumization of ΔF with respect to λ_L as

$$\sigma^* \equiv \frac{\sigma}{k_B T} = \frac{1}{n}\left[\frac{\lambda_L}{1+2S} - \frac{1}{(1-S)\phi\lambda_L^2}\right]. \tag{10}$$

The expression of η in terms of S and ϕ is obtained by minimizing ΔF with respect to $\psi(\theta)$ as

$$\eta = n_m \nu \phi_m S - \frac{n_m}{\phi_m}\left[\left(\frac{\partial \Delta F_{\mathrm{el}}}{\partial S}\right)_\phi + \left(\frac{\partial \Delta F_{\mathrm{ext}}}{\partial S}\right)_\phi\right], \tag{11}$$

where

$$\left(\frac{\partial \Delta F_{\mathrm{el}}}{\partial S}\right)_\phi = \frac{\phi}{n}\left[\frac{-\lambda_L^2}{(1+2S)^2} + \frac{1}{(1-S)^2\phi\lambda_L} - \frac{1+5S}{(1+2S)(1-S)}\right] + \frac{\phi}{n}\left[\frac{\lambda_L}{1+2S} - \frac{1}{(1-S)\phi\lambda_L^2}\right]\left(\frac{\partial \lambda_L}{\partial S}\right)_\phi, \tag{12a}$$

$$\left(\frac{\partial \Delta F_{\mathrm{ext}}}{\partial S}\right)_\phi = -\phi\sigma^*\left(\frac{\partial \lambda_L}{\partial S}\right)_\phi, \tag{12b}$$

and

$$\left(\frac{\partial \lambda_L}{\partial S}\right)_\phi = \frac{(1-S)[\phi(1-S)\lambda_L^3 + 2(1+2S)]}{2n\sigma^*(1-S)^2\lambda_L^3 + 3\lambda_L}. \tag{12c}$$

The swelling is equilibrated by the balance of the chemical potentials of the solvents inside and outside the gel (designated as μ and μ^o, respectively),

$$\frac{\mu - \mu^o}{k_B T} = 0. \tag{13}$$

The condition for equilibrium swelling is obtained from Eq. (13) as

$$\frac{1}{n}\left[\frac{1}{\lambda_L} + \phi^2\left(\frac{1}{\phi\lambda_L^2} - \frac{\lambda_L}{1+2S}\right)\left(\frac{\partial \lambda_L}{\partial \phi}\right)_S\right] + \ln(1-\phi) + \phi + \chi\phi^2 + \tfrac{1}{2}\nu\phi_m^2 S^2 + \phi^2\sigma^*\left(\frac{\partial \lambda_L}{\partial \phi}\right)_S = 0, \tag{14}$$

where

$$\left(\frac{\partial \lambda_L}{\partial \phi}\right)_S = -\frac{\lambda_L(1+2S)}{\phi[\lambda_L^2\phi(1-S) + 2(1+2S)]}. \tag{15}$$

The equilibrium values of λ_L. ϕ, and S as functions of T and σ^* are obtained as the solutions satisfying Eqs. (7), (10), and (14) simultaneously.

III. THEORETICAL RESULTS

Figures 1(a) and 1(b) show the theoretical Q-T and λ-T curves under various stresses, respectively. Figure 1(c) illustrates the corresponding T dependence of S. The temperature in the figure is reduced by the transition temperature T_{NI}^0 in the case of $\sigma^*=0$ (free swelling). The employed large value of $\nu/\chi(=10^4)$ corresponds to the case of good solvents. The

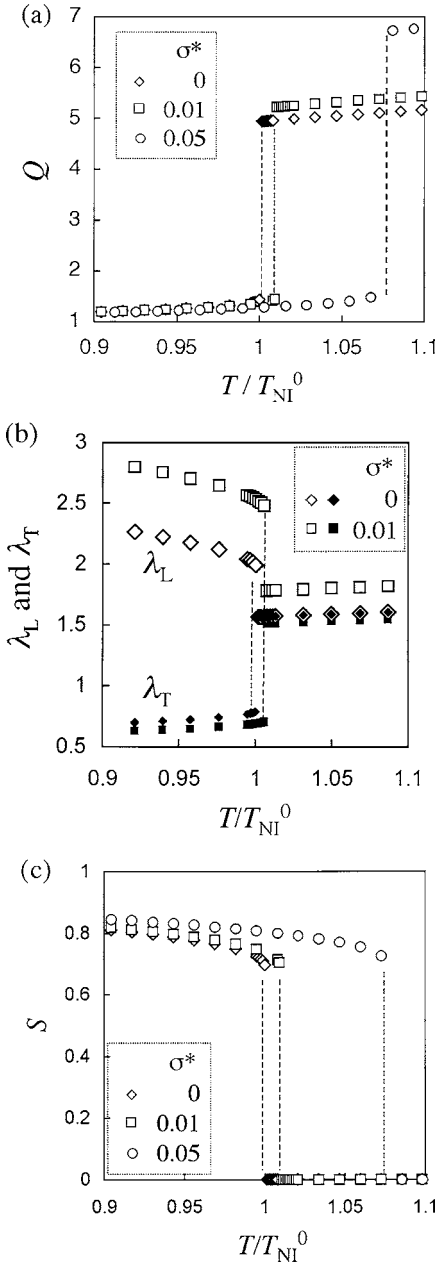

FIG. 1. The theoretical temperature dependence of (a) the degree of swelling, (b) principal ratios, and (c) orientational order parameter under various loadings. The temperature is reduced by the transition temperature in the unloaded state. The parameters used in the calculation are $n=50$, $\nu/\chi=0.05$, $p=0.3$, and $n_m=3$.

elastomers without loading are highly swollen in the high-temperature isotropic state ($S=0$), whereas they are shrunken in the low-temperature nematic state ($S>0$). Even in the case of $\sigma^*=0$, the swelling in the nematic state is anisotropic ($\lambda_L>\lambda_T$). Figure 1 indicates the two major features of the loading effect on swelling: (i) the loading shifts T_{NI} to higher temperatures as a result of the stabilization of the orientational order, and the shift increases with loading: (ii) the loading induces further swelling in the isotropic state whereas it has no appreciable effect on the volume in the nematic state.

The following osmotic Poisson's ratio (μ_{os}) is a useful parameter to estimate the degree of stress-induced swelling:

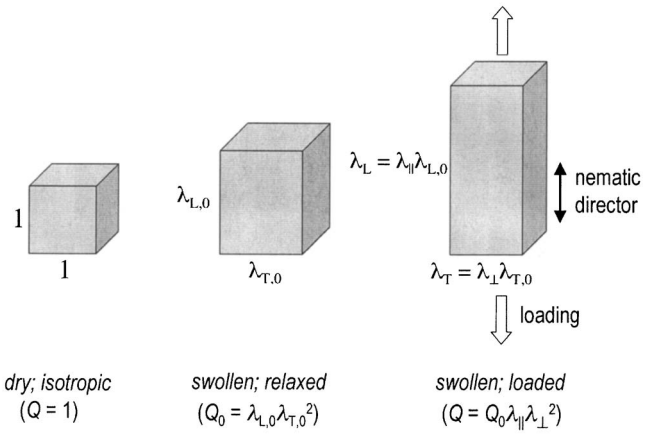

FIG. 2. Relations between λ_L, λ_T, $\lambda_\parallel$, and $\lambda_\perp$.

$$\mu_{os} = -\frac{\varepsilon_\perp}{\varepsilon_\parallel} = -\frac{\ln \lambda_\perp}{\ln \lambda_\parallel}, \tag{16}$$

where $\varepsilon_\parallel$ and $\lambda_\parallel$ are the true strain and principal ratio along the director in the loaded state measured from the *swollen state before loading*, $\varepsilon_\perp$ and $\lambda_\perp$ are the corresponding quantities normal to the director ($\lambda_\parallel = \lambda_\perp = 1$ in the unloaded and swollen state). Figure 2 illustrates the relations between $\lambda_\parallel$, $\lambda_\perp$, λ_L, and λ_T, and they are written as $\lambda_\parallel = \lambda_L/\lambda_{L,0}$ and $\lambda_\perp = \lambda_T/\lambda_{T,0}$, where the subscript 0 denotes the swollen and relaxed state. The value of μ_{os} is a direct measure of the stretching-induced volume change (ΔV_{os}): $\mu_{os} = 1/2$ when $\Delta V_{os} = 0$; μ_{os} becomes less than 1/2 when $\Delta V_{os} > 0$; and $\mu_{os} > 1/2$ in the case of $\Delta V_{os} < 0$. Figure 3 displays the theoretical T dependence of $\lambda_\parallel$, $\lambda_\perp$, and μ_{os} for the same conditions as in Figure 1. Both λ and μ_{os} primarily depend on whether the state of interest is isotropic or nematic, almost independently of T within each phase excepting the vicinity of T_{NI}. In the isotropic state, $\mu_{os}(\approx 0.3)$ is definitely smaller than 1/2 as a result of induced swelling. The value of μ_{os} for isotropic gels in the good solvent limit was derived by several theories,[19,35,36] and it ranges from 1/6 to 1/4. In the present theory, μ_{os} in the isotropic state considerably depends on χ and n, and it approaches 1/4 when the values of ν/χ and n are sufficiently high. In contrast, μ_{os} in the nematic state is close to or slightly larger than 1/2, and the value is insensitive to the theoretical parameters such as ν/χ and n_m. The theory expects that the stretching induces no volume change or a slight shrinkage in the nematic state. In the framework of the present theory, each value of μ_{os} in the isotropic or nematic state is independent of σ^*.

IV. EXPERIMENTS

A. Sample preparation

A film specimen of side chain LCE was prepared by the method described in Ref. 11. The mesogenic monomer, solvent, cross-linker, and initiator for photopolymerization were the same as those employed in the previous study. The cross-linker concentration was 10 mol % in the feed. After the cross-linking reaction, the LCE film was allowed to swell in dichloromethane to wash out the unreacted materials. The dried rectangular sample strips of 50 mm in length and 2 mm in width with a thickness of 50 μm was employed as the specimen. Di-*n*-amylphthalate was used as the solvent for swelling experiments.

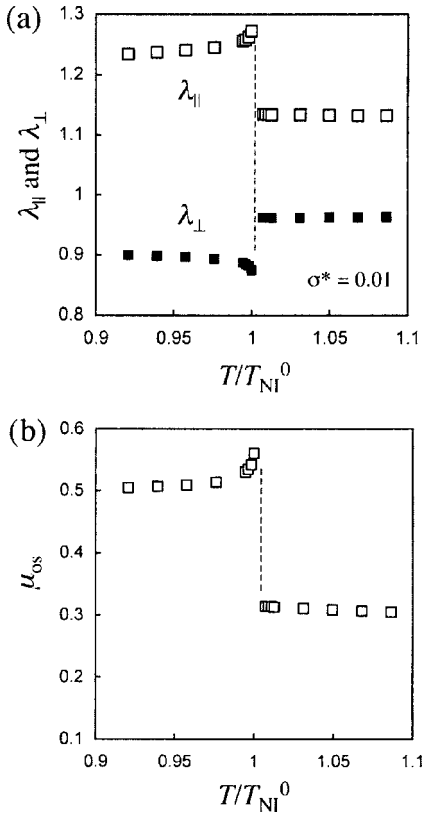

FIG. 3. The theoretical temperature dependence of (a) principal ratios and (b) osmotic Poisson's ratio under $\sigma^* = 0.01$. The temperature is reduced by the transition temperature in the unloaded state. The parameters used in the calculation are the same as those in Fig. 1.

B. Measurements

The experimental setup is schematically shown in Fig. 4. The loading on the swollen sample was imposed by suspending a weight of known mass from the end of the sample strip. The loading direction was parallel to the initial director. The swelling temperature was controlled by temperature-controlled circulating water with a custom-built double jacket bath. The swelling process was recorded by a charge coupled device camera, and the sample dimensions (d) were

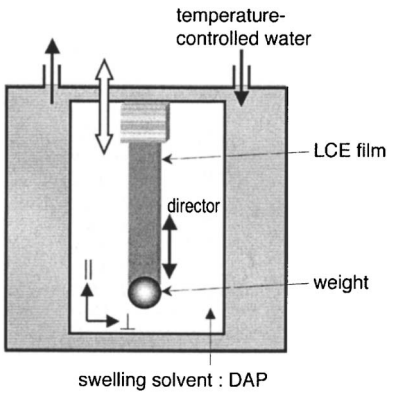

FIG. 4. The experimental setup for the swelling under constant loads.

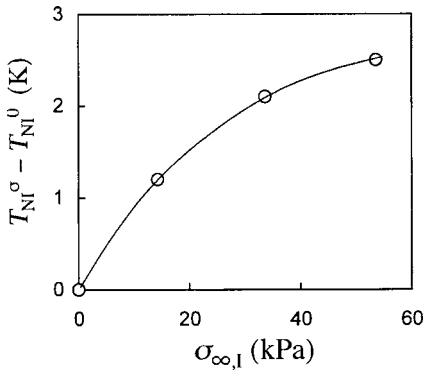

FIG. 5. The shift of the transition temperature caused by loadings as a function of imposed stress. The stress is the force per cross section in the isotropic state of $T=T_{\mathrm{NI}}^{\sigma}+5\ ^{\circ}\mathrm{C}$, where T_{NI}^{σ} is the transition temperature in the loaded state.

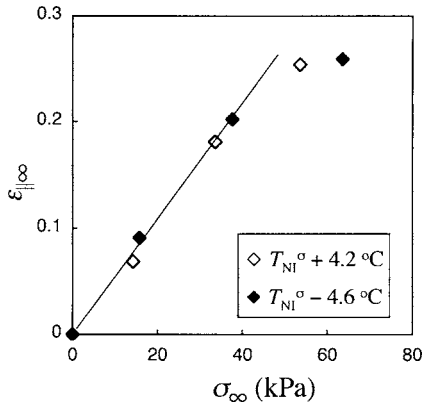

FIG. 6. The equilibrium true strain in the director direction as a function of imposed stress (the force per cross section in the loaded and steady state) in the nematic and isotropic states.

measured by the video analysis. The principal ratios $\lambda_{\parallel}$ and $\lambda_{\perp}$ were obtained from $\lambda_{\parallel}=d_{\parallel}/d_{\parallel,0}$ and $\lambda_{\perp}=d_{\perp}/d_{\perp,0}$, respectively. The degree of swelling (Q), i.e., the ratio of the volume in the swollen state (V) to that in the dry and isotropic state (V_{dry}), was evaluated as $Q=V/V_{\mathrm{dry}}=d_{\parallel}d_{\perp}^{2}/(d_{\parallel,\mathrm{dry}}d_{\perp,\mathrm{dry}}^{2})$.

The swelling in the unloaded state was achieved by lowering sufficiently the sample position so that the pendant weight could lie on the bottom of the bath. After the swelling was equilibrated in the unloaded state, the loads were imposed by raising the sample position so that the weights could be pending apart from the bath bottom. The nematic-isotropic transition temperature (T_{NI}^{σ}) in the loaded state was estimated by the observation using the crossed polarizers. In the measurements of T_{NI}^{σ}, the temperature near T_{NI}^{σ} was carefully stepwise reduced from the isotropic state after confirming the swelling equilibration at each temperature. The stress-induced swelling experiments under various loadings were carried out at the two temperatures, i.e., 53.7 and 44.9 °C, in the isotropic and nematic states.

V. EXPERIMENTAL RESULTS AND DISCUSSION

Figure 5 shows the shift of the transition temperature ($T_{\mathrm{NI}}^{\sigma}-T_{\mathrm{NI}}^{0}$) as a function of imposed stress $\sigma_{\infty,1}$ where $\sigma_{\infty,1}$ is the true stress, i.e., the force per cross section in the swollen and loaded state at 55 °C [$=T_{\mathrm{NI}}^{0}+8\ ^{\circ}\mathrm{C}$, where T_{NI}^{0} (47 °C) is the transition temperature in the swollen state without loading]. The transition temperature increases with loading along the director as a result of the stabilization of the nematic state. This trend is the same as the theoretical prediction in Fig. 2. The similar loading effects on T_{NI} were also observed in the neat state of LCEs.[2]

Figure 6 illustrates the equilibrium strain $\varepsilon_{\parallel\infty}$ as a function of imposed stress in the isotropic and nematic states. The stress in the figure is the force per cross section in the loaded state. The data points at the largest stress seem to deviate from the linear relation owing to the nonlinear effect. There is no appreciable difference in the initial Young's modulus (approximately 200 kPa) between the isotropic and nematic states. Several studies reported that the corresponding difference in the neat LCEs was also small, and it was less than 15% within the temperature range of $T_{\mathrm{NI}}-10\ ^{\circ}\mathrm{C}<T<T_{\mathrm{NI}}+10\ ^{\circ}\mathrm{C}$.[37,38] As the first approximation for isotropic elastomers, the swelling changes the modulus by a factor of $Q^{-1/3}$.[39] The swelling effect on the modulus in the present study is small because the ratio of Q in the isotropic and nematic states is as large as 2.

Figure 7 displays the time (t) dependencies of the principal ratios ($\lambda_{\parallel}$ and $\lambda_{\perp}$) and volume (Q) after the imposition of the stress at $t=0$. Before loading, the isotropic elastomer at 53.7 °C ($=T_{\mathrm{NI}}^{\sigma}+4.2\ ^{\circ}\mathrm{C}$) is in the swollen state, while the nematic elastome at 44.9 °C ($=T_{\mathrm{NI}}^{\sigma}-4.6\ ^{\circ}\mathrm{C}$) is in the shrunken state, which can be seen in Fig. 7(c). The stress imposition results in the instantaneous uniaxial stretching along the director at $t=0$: approximately 26% elongation in the loading direction and approximately 10% shrinkage in its normal directions under this loading. This instantaneous deformation corresponds to the uniaxial stretching of incompressible elastomers ($\mu=1/2$), as described later. At long times, both principal ratios gradually increase with time in the isotropic state, while $\lambda_{\parallel}$ slowly increases but with no appreciable change in $\lambda_{\perp}$ in the nematic state. It should be emphasized that these shape variations in the long time region are due to neither of the viscoelastic creep effect nor plastic flow, because the time scale of the phenomena is explained by the diffusion of polymer networks as mentioned later, and the shape recovers the original state after unloading in the similar time scale. Figure 7(c) shows the corresponding change in volume. The degree of swelling Q in the loaded state is given by $Q=Q_0\lambda_{\parallel}\lambda_{\perp}^{2}$. The magnitude of the stress-induced swelling $|(Q-Q_0)/Q_0|$ in the isotropic state (approximately 0.11) is definitely larger than that in the nematic state (approximately 0.02). The results in Fig. 7 shows that the loading induces a finite further swelling but the induced swelling significantly differ in the degree and anisotropy between the isotropic and nematic states.

The osmotic Poisson's ratio μ_{os} defined by Eq. (16) is a convenient parameter to characterize the induced swelling. Figure 8 illustrates the time dependence of μ_{os} under various loads in the nematic and isotropic states. At short times at $t\approx 0$, μ_{os} is close to 0.5, i.e., the materials behave as incompressible materials such as conventional elastomers. The equilibrium values of μ_{os} in the long time limit slightly depends on the imposed load, but they primarily depend on whether the state of interest is isotropic or nematic. In the

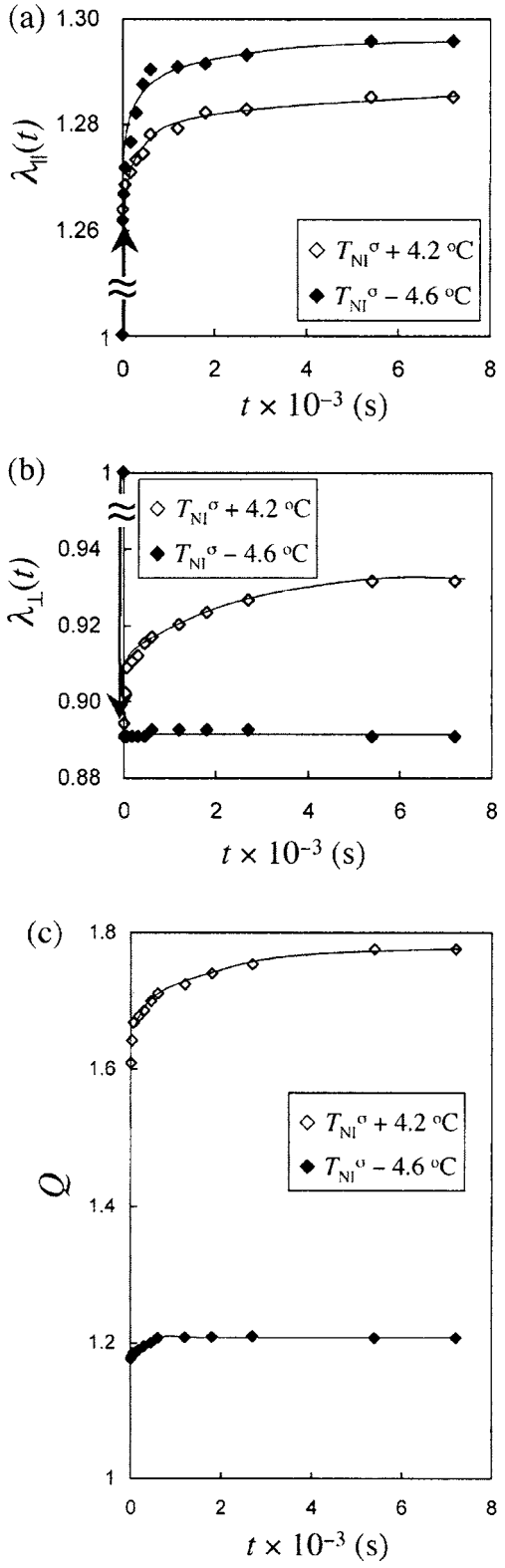

FIG. 7. The time dependence of the principal ratios (a) along and (b) normal to the director; (c) the degree of swelling after imposing the constant load in the isotropic and nematic states. The imposed constant load corresponds to σ=53.6 and 63.6 kPa (the force per cross section in the steady state) in the isotropic and nematic states, respectively.

isotropic state, the equilibrium values of μ_{os} are approximately 0.25 as a result of the pronounced stress-induced swelling. These equilibrium values are similar to those[22,27] reported for the isotropic gels swollen in good solvents as

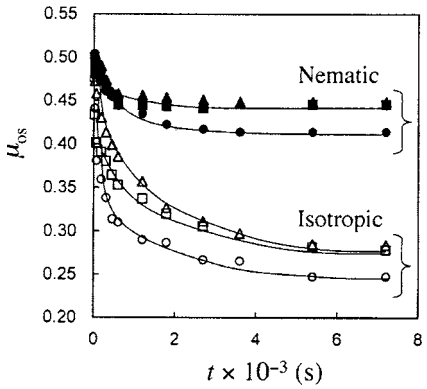

FIG. 8. The time dependence of osmotic Poisson's ratio for various loadings. The open circular, triangular, and rectangular symbols depict the data in the isotropic state for σ=14.2, 33.6, and 53.6 kPa (the force per cross section in the steady state at 53.7 °C), respectively. The closed circular, triangular, and rectangular symbols represent the data in the nematic state for σ=15.7, 37.6, and 63.6 kPa (the force per cross section in the steady state at 44.9 °C), respectively.

well as the theoretical value in Fig. 3. The equilibrium values of μ_{os} in the nematic state lie around 0.45, close to 1/2 and definitely larger than those in the isotropic state. This is a direct consequence of no considerable induced swelling in the nematic state. The different reswelling behaviors observed are schematically illustrated in Fig. 10.

The theory predicts μ_{os} in the nematic state to be approximately 0.5 as a result of almost no loading effect on swelling at the temperatures of $T/T_{NI}^{0}<0.99$ (Fig. 3). The theoretical values of μ_{os} are slightly larger from those in the experiments at the temperature of $T/T_{NI}^{0}\approx 0.98$, but the theory qualitatively describes the difference in the stress-induced swelling behaviors in the isotropic and nematic states. The present model should be further improved for the quantitative description, especially for the behavior in the isotropic state. If the prediction is fitted to the swelling data ($Q\approx 1.7$) in the isotropic state, the corresponding theoretical $\mu_{os}(>0.4)$ disagrees with the data. Conversely, the condition of $\mu_{os}=1/4$ leads to the markedly high swelling in the isotropic state ($Q>30$). These are mainly due to the oversimplification of the mixing interaction parameter χ for the networks composed of rigid and flexible units. The introduction

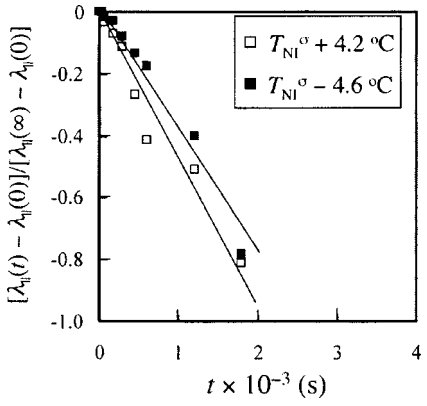

FIG. 9. Semilog plot of the reduced change in $\lambda_{\parallel}$ vs time in the isotropic and nematic states. The imposed stresses are 14.2 and 15.7 kPa (the force per cross section in the steady state) in the isotropic and nematic states, respectively.

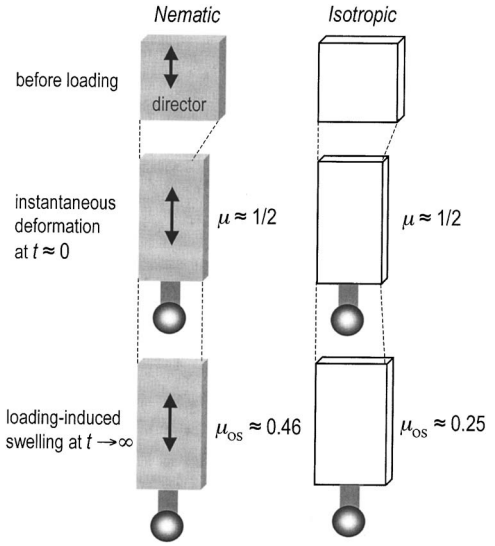

FIG. 10. Schematics for the observed loading-induced swelling in the nematic and isotropic states.

of several mixing interaction parameters for each component/solvent and the different components improves the quality of the fitting but the most essential feature in this phenomenon, i.e., the role of nematic order in stress-induced swelling, becomes obscure by the complexity. The theory also overestimates the shape anisotropy ($\lambda_{\parallel}/\lambda_{\perp}$) in the nematic state, which was observed in the previous study.[8] This results from the overestimation of S from the Maier-Saupe approach. More quantitative theoretical description will be developed on the basis of the present model.

The different reswelling behaviors in the isotropic and nematic states can be qualitatively understood by considering which the system favors, the isotropic or oriented state: In the high-temperature isotropic state, the further swelling occurs in order to reduce the shape anisotropy that is caused by imposed elongation. In the low-temperature nematic state, the loading stabilizes the nematic state because of a further growth of orientational order. The swelling that acts to decrease the orientational order is not thermodynamically favored in the nematic state. For instance, in the previous study on the free-swelling of nematic elastomers in isotropic solvents.[8] the degree of swelling remains almost unchanged when the temperature is reduced, i.e., the nematic order increases. However, if the solvent also has the nematicity, the loading effect may be substantially different from that in the isotropic solvent systems. The nematic orders of the solvents inside and outside LCEs also play an important role in anisotropic swelling as observed in the free swelling.[9,11] The loading effect in the nematic solvent systems is an interesting issue for future study.

Figure 9 displays the semilog plots of $\Delta\lambda_{\parallel}(t)$ versus time in the isotropic and nematic states where $\Delta\lambda_{\parallel}(t)=\lambda_{\parallel\infty}-\lambda_{\parallel}(t)$ and $\lambda_{\parallel\infty}$ is the equilibrium value of $\lambda_{\parallel}$. As the data points appear to fall on the straight line passing through the origin, the kinetics is approximated by a single exponential relaxation. From the inverse of the slope, the characteristic time (τ) is estimated to be 1.1×10^{2} and 9.1×10^{2} s in the nematic and isotropic states, respectively. The diffusion constant (D) is approximately evaluated to be 3.0×10^{-12} and 3.1×10^{-12} m^2/s in the nematic and isotropic states, respectively, from $D\approx d_{\infty}^2/\tau$, where d_{∞} is the equilibrium thickness of the elastomer film. In the present specimen having the thickness less than 10% of other dimensions, the thickness is the effective dimension governing the diffusion of networks. The values of D in the nematic and isotropic states are comparable, and they are in the same order of the reported values of D for the isotropic gels.[19,40] The latter confirms that these shape variations result from the swelling process, not from the viscoelastic creep effect.

VI. CONCLUSIONS

The effects of externally imposed loading on the swelling of nematic elastomers are significantly different in the high-temperature isotropic and low-temperature nematic states. In the isotropic state, the stretching induces a further swelling, which is similar to conventional isotropic elastomers. In contrast, in the nematic state, the stretching-driven volume change is significantly suppressed. In terms of osmotic Poisson's ratio (μ_{os}). $\mu_{os}\approx0.30$ in the isotropic state and $\mu_{os}\approx0.45$ in the nematic state. The different reswelling behaviors under stretching in the isotropic and nematic states are qualitatively described by a mean field theory. In the isotropic state, the system thermodynamically favors the less anisotropic state, and the further swelling acts to decrease the shape anisotropy that arises from imposed loading. In the nematic state, the loading stabilizes the nematic phase as a result of an increase in nematic order, and it does not lead to further swelling that reduces the orientational order.

ACKNOWLEDGMENTS

This work was partly supported by the Grant-in-Aid for Scientific Research (B) (No. 16750186) and that on Priority Area "Soft Matter Physics" (No. 19031014) from the Ministry of Education, Culture, Sports, Science and Technology of Japan.

[1] P. G. de Gennes, C. R. Seances Acad. Sci., Ser. B **281**, 101 (1975).
[2] M. Warner and E. M. Terentjev, *Liquid Crystals Elastomers* (Clarendon, London, 2003).
[3] P. Xie and R. J. Zhang, J. Mater. Chem. **15**, 2529 (2005).
[4] H. R. Brand, H. Pleiner, and P. Martinoty, Soft Matter **2**, 182 (2006).
[5] K. Urayama, Macromolecules **40**, 2277 (2007).
[6] J. Kupfer and H. Finkelmann, Makromol. Chem., Rapid Commun. **12**, 717 (1991).
[7] K. Urayama, Y. Okuno, and S. Kohjiya, Macromolecules **36**, 6229 (2003).
[8] K. Urayama, Y. O. Arai, and T. Takigawa, Macromolecules **38**, 3469 (2005).
[9] K. Urayama, Y. Okuno, T. Nakao, and S. Kohjiya, J. Chem. Phys. **118**, 2903 (2003).
[10] Y. Yusuf, Y. Ono, Y. Sumisaki, P. E. Cladis, H. R. Brand, H. Finkelmann, and S. Kai, Phys. Rev. E **69**, 021710 (2004).
[11] K. Urayama, Y. O. Arai, and T. Takigawa, Macromolecules **38**, 5721 (2005).
[12] R. Vendamme and U. Maschke, e-Polymers 069 (2006).
[13] M. Warner and X. J. Wang, Macromolecules **25**, 445 (1992).
[14] X. J. Wang and M. Warner, Macromol. Theory Simul. **6**, 37 (1997).
[15] A. Matsuyama and T. Kato, J. Chem. Phys. **114**, 3817 (2001).
[16] A. Matsuyama and T. Kato, J. Chem. Phys. **116**, 8175 (2002).
[17] K. Urayama, Y. O. Arai, and T. Takigawa, Macromolecules **37**, 6161 (2004).

[18] K. Urayama, R. Mashita, Y. O. Arai, and T. Takigawa, Macromolecules **39**, 8511 (2006).
[19] T. Takigawa, K. Urayama, Y. Morino, and T. Masuda, Polym. J. (Tokyo, Jpn.) **25**, 929 (1993).
[20] P. Chiarelli, P. J. Basser, D. Derossi, and S. Goldstein, Biorheology **29**, 383 (1992).
[21] T. Yamauc and M. Doi, J. Chem. Phys. **122**, 084703 (2005).
[22] T. Takigawa, Y. Morino, K. Urayama, and T. Masuda, Polym. J. (Tokyo, Jpn.) **28**, 1012 (1996).
[23] S. Vervoort, S. Patlazhan, J. Weyts, and T. Budtova, Polymer **46**, 121 (2005).
[24] K. Urayama, T. Takigawa, and T. Masuda, Rheol. Acta **33**, 89 (1994).
[25] T. Takigawa, K. Uchida, K. Takahashi, and T. Masuda, J. Chem. Phys. **111**, 2295 (1999).
[26] K. Urayama, S. Okada, S. Nosaka, H. Watanabe, and T. Takigawa, J. Chem. Phys. **122**, 024906 (2005).
[27] S. Nosaka, K. Urayama, and T. Takigawa, Polym. J. (Tokyo, Jpn.) **37**, 694 (2005).
[28] F. Weiss and H. Finkelmann, Macromolecules **37**, 6587 (2004).
[29] H. W. Chiu and T. Kyu, J. Chem. Phys. **103**, 7471 (1995).
[30] H. W. Chiu, Z. L. Zhou, T. Kyu, L. G. Cada, and L. C. Chien, Macromolecules **29**, 1051 (1996).
[31] M. Warner, K. P. Gelling, and T. A. Vilgis, J. Chem. Phys. **88**, 4008 (1988).
[32] P. J. Flory, *Principles of Polymer Chemistry* (Cornell University Press, Ithaca, NY, 1953).
[33] W. Maier and A. Saupe, Z. Naturforsch. A **14A**, 882 (1959).
[34] P. G. de Gennes and J. Prost, *The Physics of Liquid Crystals*, 2nd ed. (Oxford University Press, New York, 1993).
[35] E. Geissler and A. M. Hecht, Macromolecules **13**, 1276 (1980).
[36] S. Alexander and Y. Rabin, J. Phys.: Condens. Matter **2**, Sa313 (1990).
[37] H. Finkelmann, A. Greve, and M. Warner, Eur. Phys. J. E **5**, 281 (2001).
[38] P. Martinoty, P. Stein, H. Finkelmann, H. Pleiner, and H. R. Brand, Eur. Phys. J. E **14**, 311 (2004).
[39] L. R. G. Treloar, *The Physics of Rubber Elasticity*, 3rd ed. (Clarendon, Oxford, 1975).
[40] T. Tanaka and D. J. Fillmore, J. Chem. Phys. **70**, 1214 (1979).